

## Effect of SiO<sub>2</sub> on Rheology, Morphology, Thermal, and Mechanical Properties of High Thermal Stable Epoxy Foam

Keping Chen, Chunrong Tian, Ai Lu, Qiuming Zhou, Xiaorong Jia, Jianhua Wang

Institute of Chemical Materials, China Academy of Engineering Physics, Mianyang 621900, China

Correspondence to: C. Tian (E-mail: tianchr1972@163.com) or J. Wang (E-mail: wjh@caep.ac.cn)

**ABSTRACT:** A series of highly thermostable epoxy foams with diglycidyl ether of bisphenol-A and bisphenol-S epoxy resin (DGEBA/DGEBS), 4,4'-diaminodiphenyl sulfone (DDS) as curing agent have been successfully prepared through a two-step process. Dynamic and steady shear rheological measurements of the DGEBA/DGEBS/DDS reacting mixture are performed. The results indicate all samples present an extremely rapid increase in viscosities after a critical time. The gel time measured by the crossover of  $\tan \delta$  is independent of frequency. The influence of SiO<sub>2</sub> content on morphology, thermal, and mechanical properties of epoxy foams has also been investigated. Due to the heterogeneous nucleation of SiO<sub>2</sub>, the pore morphology with a bimodal size distribution is observed when the content of SiO<sub>2</sub> is above 5 wt %. Dynamic mechanical analysis (DMA) reveals that pure epoxy foam possesses a high glass transition temperature (206°C). The maximum of specific compressive strength can be up to 0.0253 MPa m<sup>3</sup> kg<sup>-1</sup> at around 1.0 wt % SiO<sub>2</sub>. © 2013 Wiley Periodicals, Inc. *J. Appl. Polym. Sci.* **2014**, *131*, 40068.

**KEYWORDS:** foams; rheology; mechanical properties; viscosity and viscoelasticity; thermal properties

Received 14 May 2013; accepted 16 October 2013

DOI: 10.1002/app.40068

### INTRODUCTION

Polymeric foams provide structural support, cushioning, energy absorption (packaging) and thermal insulation in critical locations, such as naval vessels, military vehicles and aircraft, etc.<sup>1–3</sup> Epoxy foam with excellent performances in moisture absorption, thermal and chemical stability and mechanical properties has remarkably broad range of applications including construction, aircraft-interior panels, crash-pads, composite foam cores, etc.<sup>4</sup>

Epoxy syntactic foam, a kind of novel structural epoxy foam, is prepared through the incorporation of hollow microballoon fillers in the polymeric binder matrices.<sup>5</sup> The characteristics of high compressive strength, low coefficient of thermal expansion and low moisture absorption lead to their use in aerospace structural materials.<sup>6</sup> However, this method cannot obtain foams with lower density, more than 0.5 g cm<sup>-3</sup> typically, and microballoon cannot be dispersed homogeneously because of different density of epoxy resin matrix.<sup>7–9</sup> Physical or chemical blowing agents could be used to obtain epoxy foams with low density. For a physical foaming process, the exothermic cross-linked reaction takes place to evaporate the low boiling solvent. Aubert<sup>10</sup> successfully incorporated Diels-Alder reversible chemistry into epoxy resins to prepare a removable epoxy foam with a physical blowing agent (Fluorinert FC-72). The glass transition temperature ( $T_g$ ) is only 85°C based on the maximum in

the mechanical loss factor ( $\tan \delta$ ) from dynamic mechanical analysis (DMA) curve. In our previous research, microwave irradiation method was used to prepare epoxy foams with water as blowing agent.<sup>11</sup>

Some reports have been published on the chemical process. Vazquez<sup>12</sup> optimized composition of the epoxy-amine reactive system to obtain epoxy foam with siloxane as chemical foaming agent. However, the maximum  $T_g$  is only 85°C, the size of bubbles is relatively large and the size distribution of bubble is broad. Short-fiber,<sup>13–15</sup> microcellulose,<sup>16</sup> and silica (SiO<sub>2</sub>)<sup>17</sup> were always used as fillers to improve the thermal and mechanical properties of epoxy foams. However, most of them focus on the composites and mechanical properties, and little attention is given to the viscosity evolution with time. Low viscosity causes coalescence and rupture of bubbles, whereas high viscosity gives rise to low porosity. In order to obtain homogeneous well-defined foam, it is necessary to understand the rheological behavior of epoxy during precuring on foaming. Recently, Koyama and colleague<sup>18</sup> determined the critical gel time of epoxy system through dynamic shear viscoelasticity test to optimize the viscosity for stable growth of foaming cell.

Therefore, in this study, a series of high thermal stable epoxy foams ( $T_g = 221^\circ\text{C}$ ) with diglycidyl ether of bisphenol-A and bisphenol-S epoxy resin (DGEBA/DGEBS), 4,4'-diaminodiphenyl sulfone (DDS) as curing agent, azodicarbonamide

(ADCA) as chemical blowing agent were prepared through a two-step process. The viscosity evolution with time of system was measured through steady and dynamic shear viscoelasticity test to optimize the precuring temperature and time. The morphology, thermal, and mechanical properties of the epoxy foams were also investigated.

## EXPERIMENTAL

### Materials

A low-molecular-weight epoxy resin, DGEBA (epoxy value = 0.51) and DGEBS (epoxy value = 0.38), were supplied by Chenguang and Yuancheng chemical plant, respectively. ADCA (decomposition temperature is 180°C) as chemical blowing agent was provided by Solvay. Silica (SiO<sub>2</sub>, D-17, the average diameter is 7 μm) was purchased from Degussa. DDS provided by Yinhua chemical plant was used as received.

### Preparation of the High Thermal Stable Epoxy Foams

The preparation of the epoxy foams were based on methods described previously. Briefly, 100 weight part of epoxy resins (DGEBA/DGEBS = 50/50 wt) were added in a 250-mL glass beaker and then placed in an oil bath preheated at 140°C. When the reactants dissolved completely, SiO<sub>2</sub> was added and the reaction was stirred mechanically at a stirring rate of 500 r min<sup>-1</sup>. After 10–30 min, 27.5 weight part of curing agent (DDS) was added gradually to precure for a certain time. 1.5 weight part of ADCA blowing agent was mixed with the system for 10 min. The precured epoxy resin was cast into an aluminum mold and then transferred into an oven at 185°C for molded foaming process. In order to ensure completion of the reaction, the obtained foams were postcured in oven at 185°C for above 4 h.

### Rheological Analysis

Dynamic oscillatory shear measurements of the resin containing 0, 1, 3, 5, and 10 wt % of SiO<sub>2</sub> were performed on a rotational rheometer (Haake RS600 Instruments) at different frequencies (1, 3, 5, and 10 Hz) and constant temperature (140°C). The sample was prepared as a weight ratio of DGEBA/DGEBS/DDS of 50/50/27.5 in the absence of blowing agent to avoid foaming process. The geometries of the test fixtures were parallel disks with a diameter of 60 mm for all measurements. The isothermal measurement was performed until the sample was cured. The steady shear viscosity,  $\eta$ , of the reacting mixture during the isothermal cure of the DGEBA/DGEBS/DDS was also determined at a shear rate of 1 s<sup>-1</sup> and temperature of 140–190°C. The low rotation speed was used to avoid a disturbance movement during curing.

### Thermal Properties

Differential scanning calorimetry (DSC) was performed by a TA Instruments Q200 differential scanning calorimeter using a sample weight of 10 mg with a heating rate of 20°C min<sup>-1</sup> over the temperature range of 30–250°C under a nitrogen atmosphere. Thermogravimetric analysis (TGA) was carried out using a TA Instrument 2050. TGA tests were performed in alumina crucibles and the sample weight in all tests was approximately 5 mg. Temperature programs were run from room temperature to

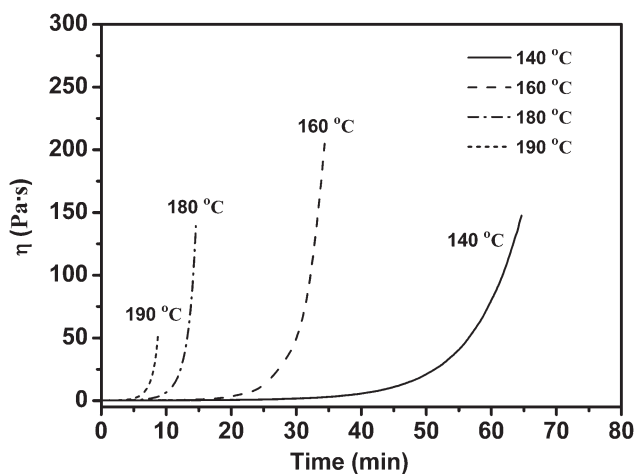


**Figure 1.** The steady shear viscosity as a function of time for pure epoxy resin cured at temperature from 140 to 190°C.

800°C at a heating rate of 10°C min<sup>-1</sup> under a nitrogen atmosphere.

### Dynamic Mechanical Analysis

Dynamic mechanical analysis (DMA) of epoxy foams was tested by Perkin-Elmer DMA 7 Series. The dimensions of the samples were 35 × 12.7 × 2 mm<sup>3</sup>. The frequency was fixed at 1 Hz. The samples were measured at a heating rate of 3°C min<sup>-1</sup> from room temperature to 250°C.

### Mechanical Properties

Compressive test was performed with an Instron 5500 machine following the standard method. The dimensions of the samples were Φ 20 mm × 20 mm (diameter and height, respectively), and at least four specimens were measured to obtain an average values. Samples were compressed between two stainless steel platens using a crosshead rate of 2.0 mm min<sup>-1</sup>. From the stress–strain curve, the compressive modulus was determined using the steepest initial slope.

### Scanning Electron Microscope

Epoxy foams morphologies were investigated with a CamScan Apollo 300 field emission scanning electron microscope (FE-SEM). For SEM analysis, samples were mounted on aluminum studs using adhesive graphite tape and sputter coated with gold before analysis. The size distribution of bubble was calculated by the Image-Pro Plus software.

## RESULTS AND DISCUSSION

### Rheological Behavior of DGEBA/DGEBS/DDS

The viscosity evolution with time plays an important role in the preparation of epoxy foam. Low viscosity causes coalescence and rupture of bubbles, whereas high viscosity gives rise to low porosity. The steady shear viscosity of DGEBA/DGEBS/DDS as a function of time, cured at temperature from 140 to 190°C, is shown in Figure 1. The results indicate that all samples show a similar tendency and possess an extremely rapid increase in viscosities after a critical time. The time up to the onset of the rapid increase in steady shear viscosity are found to be about 52, 30, 12, and 7 min at 140, 160, 180, and 190°C, respectively. It is clear that the crosslinking reaction rate is too fast to match

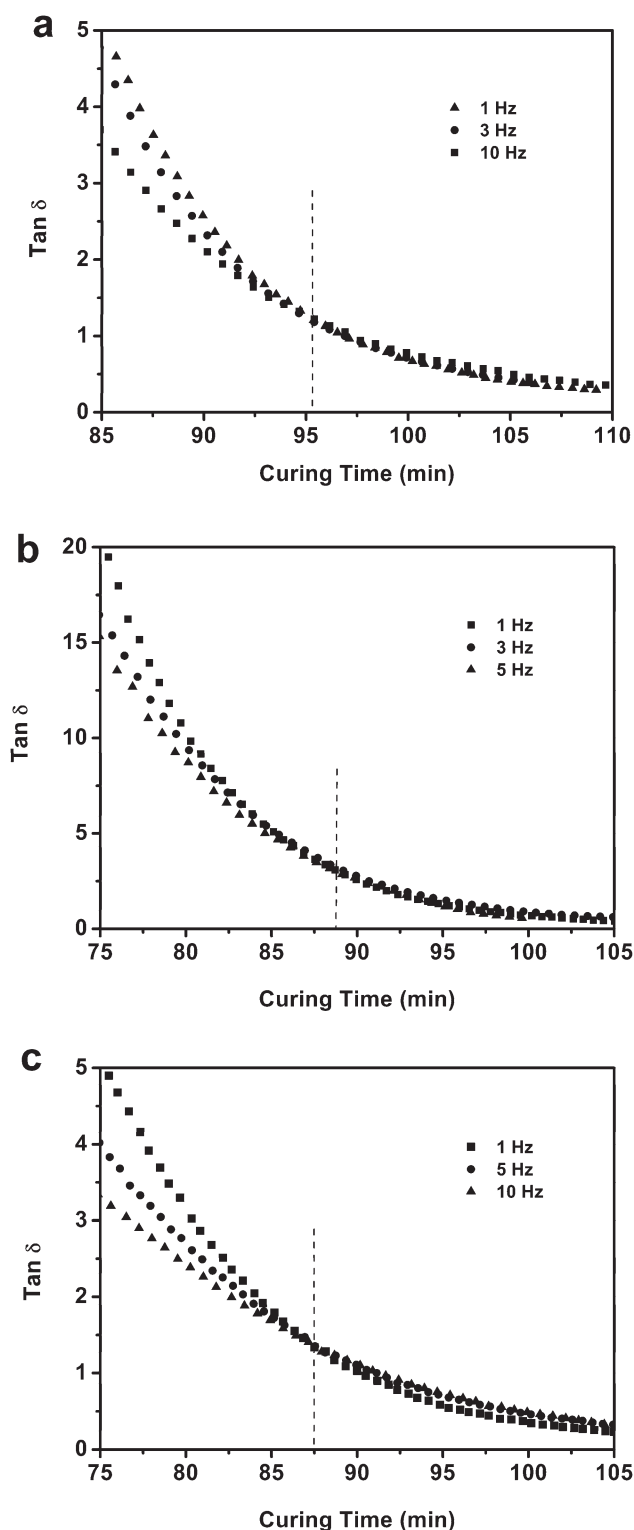


**Figure 2.** Variation in  $\tan \delta$  during cure of a DGEBA/DGEBS/DDS system at different frequency with various silica content. (a) 0% SiO<sub>2</sub>, (b) 1% SiO<sub>2</sub>, and (c) 5% SiO<sub>2</sub>.

subsequent foaming process when the precured temperature is above 160°C. Therefore, the optimum precured temperature is found to be 140°C, which is determined in terms of the stability of epoxy precured reaction. When the precured time exceeds

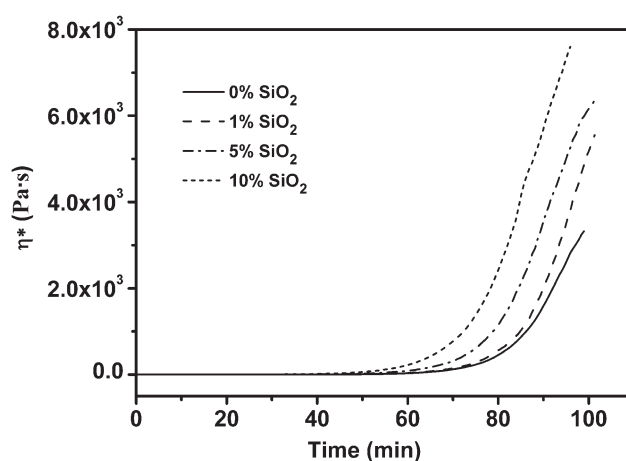


**Figure 3.** Complex viscosity ( $\eta^*$ ) as a function of time for epoxy resin cured with various silica content at 140°C.

50 min, the viscosity is suitable to lock-in the bubbles to form well-defined pore structure.

Accurate knowledge of the gel point plays an important role in the optimal temperature and time for which the sample should be heated before being allowed to set in the mold. The crossover point of the shear modulus, storage ( $G'$ ) and loss ( $G''$ ) modulus, can be effectively used to determine the gel point of some polymers.<sup>19–22</sup> However, this can only be effectively used for some specific polymers, and the type of those polymers was given by the Winter's criterion.<sup>23</sup> Boey has reported that the crossover of  $G'$  and  $G''$  of the epoxy/anhydride system was frequency dependent, the  $G'$ ,  $G''$  crossover points occurred later with increasing frequency. However, using the point where  $\tan \delta$  was found independent of the frequency can accurately define the gel point.<sup>24</sup> To determine the gel point of DGEBA/DGEBS/DDS system, dynamic rheology measurements of the resin containing various SiO<sub>2</sub> concentrations were performed at different frequencies. Figure 2 shows the evolution of  $\tan \delta$  during cure of a DGEBA/DGEBS/DDS system at different frequency (1, 3, 5, and 10 Hz) with various silica contents at 140°C. The results clearly show that the  $\tan \delta$  curves with different frequencies intersect at only one point, at which  $\tan \delta$  becomes independent of the frequency (Figure 2). Therefore, the crossover of the  $\tan \delta$  curves at various frequencies can be defined as the gel point for the system. Those results agree well with previous literature.<sup>24</sup>

From the Figure 2(a–c), the gel points of epoxy system with 0, 1, and 5 wt % SiO<sub>2</sub> are about 96, 89, and 87 min, respectively. That is, the gel points decrease with increasing the concentration of SiO<sub>2</sub> (0–5 wt %), which indicates that the SiO<sub>2</sub> will accelerate the reaction of system because of the amino silane coupling agent modified on the surface of SiO<sub>2</sub> particle. Figure 3 shows the curves of complex viscosity  $\eta^*$  as a function of time for sample with various SiO<sub>2</sub> contents, which presents the similar tendency of steady shear viscosity in Figure 1. It is clear that the critical time of an extremely rapid increase in viscosities decreases with increasing SiO<sub>2</sub> content, which accords with the data of gel point.

#### Morphology and Mechanical Properties

A series of epoxy foams with different density and SiO<sub>2</sub> content were prepared through precuring and foaming process. Figure 4

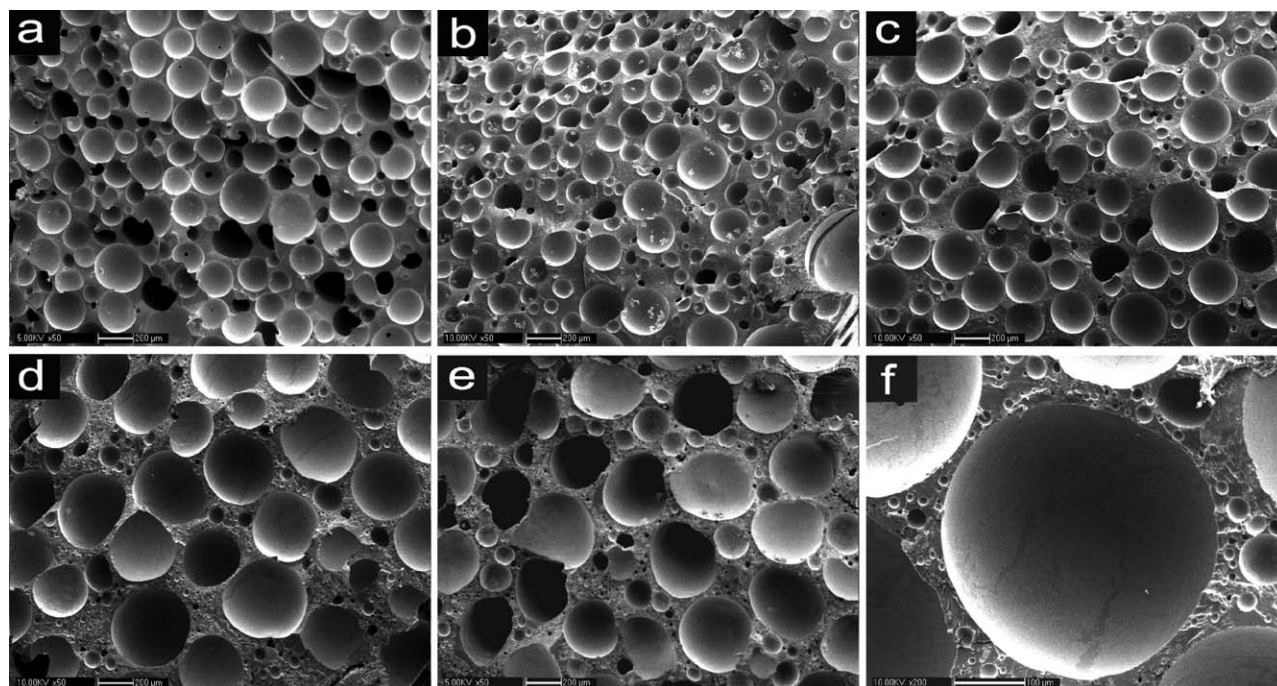


**Figure 4.** SEM morphologies and bubble size distribution of epoxy foams with different SiO<sub>2</sub> contents. The density range is 330–363 kg m<sup>-3</sup>. (a) pure epoxy foam, (b) 1 wt %, (c) 3 wt %, (d) 5 wt %, (e) 10 wt %, and (f) zoom image with 5 wt % SiO<sub>2</sub>.

shows the SEM images of the pure and filled epoxy foams with various amounts of SiO<sub>2</sub>. The variation in the bubble size distribution of epoxy foam is shown in Figure 5. When filled with 1 wt % SiO<sub>2</sub>, the average bubble size decreases abruptly and the distribution becomes narrow. This phenomenon may be explained that the incorporation of SiO<sub>2</sub> into the basic system produces a nucleating effect during foaming process, and increases the number of bubbles per volume unit. However, the distribution of cell size becomes broader with 3 wt % SiO<sub>2</sub> (Figure 5). Interestingly, when the content of SiO<sub>2</sub> is above

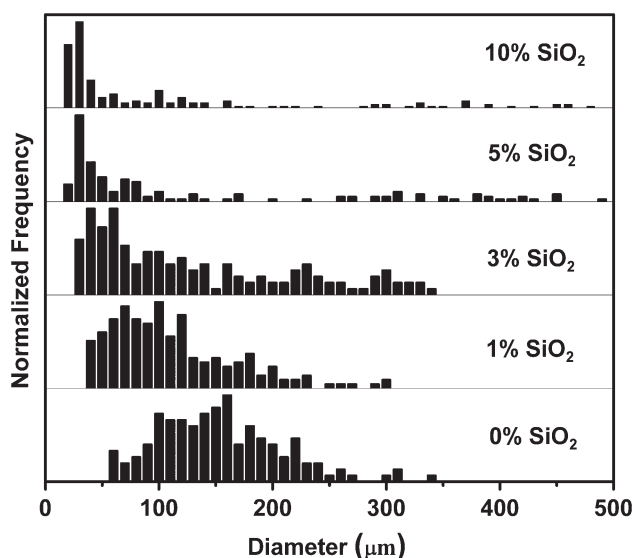


**Figure 5.** Bubble size distribution of epoxy foams with different SiO<sub>2</sub> contents.

5 wt %, the pore morphology with a bimodal size distribution is observed [Figure 4(f)], which could be explained by qualitative thermodynamic approach. Due to the heterogeneous nucleation of SiO<sub>2</sub>, bubbles are formed firstly on the surface of SiO<sub>2</sub>. At this time, the matrix is just like a kind of macroemulsion, which is thermodynamically unstable, and the bubbles will grow gradually.<sup>25,26</sup> However, owing to an excess of heterogeneous nucleating point, some adjacent bubbles would diffuse, contact together, and collapsed to form large bubbles because of interfacial tension. With the intensification of the curing process, the viscosity of system increased dramatically, and then the uncollapsed smaller cells and collapsed large cells are solidified gradually to form the bimodal size distribution, that is, large cells are surrounded by much smaller cells.

Table I shows the mechanical properties in compression for the pure and SiO<sub>2</sub> filled epoxy foams. To investigate the influence of filler on mechanical properties, the specific properties (property/density) of epoxy foams were calculated. Interestingly, when the content of SiO<sub>2</sub> is 1%, the specific strength remarkably increases by 42.9%. However, with sequentially increasing the content of SiO<sub>2</sub>, a slight decrease in the specific strength is observed, which is contrary to previous reports.<sup>17</sup> This phenomenon is due to the pore structure of epoxy foams as shown in Figures 4 and 5. In previous reports,<sup>27–30</sup> it has been demonstrated that a small cell size, low voids fraction, and high filler content can improve the compression mechanical properties. A nucleating effect during foaming process with 1 wt % SiO<sub>2</sub> decreases the average cell size, and results in the improvement in mechanical properties. However, the specific compressive strength decreases when increasing SiO<sub>2</sub> content, this is because those large cells in the matrix will be crush firstly by external



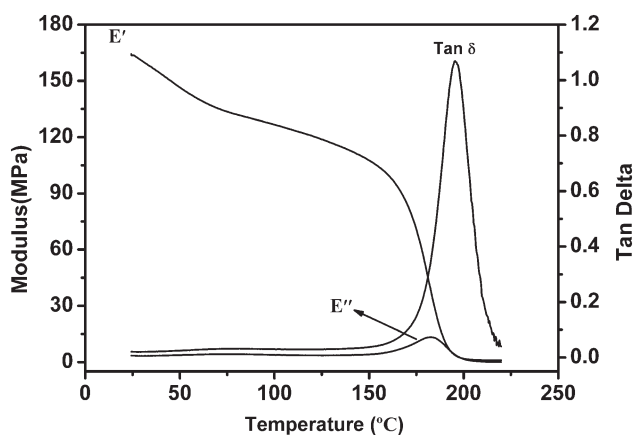
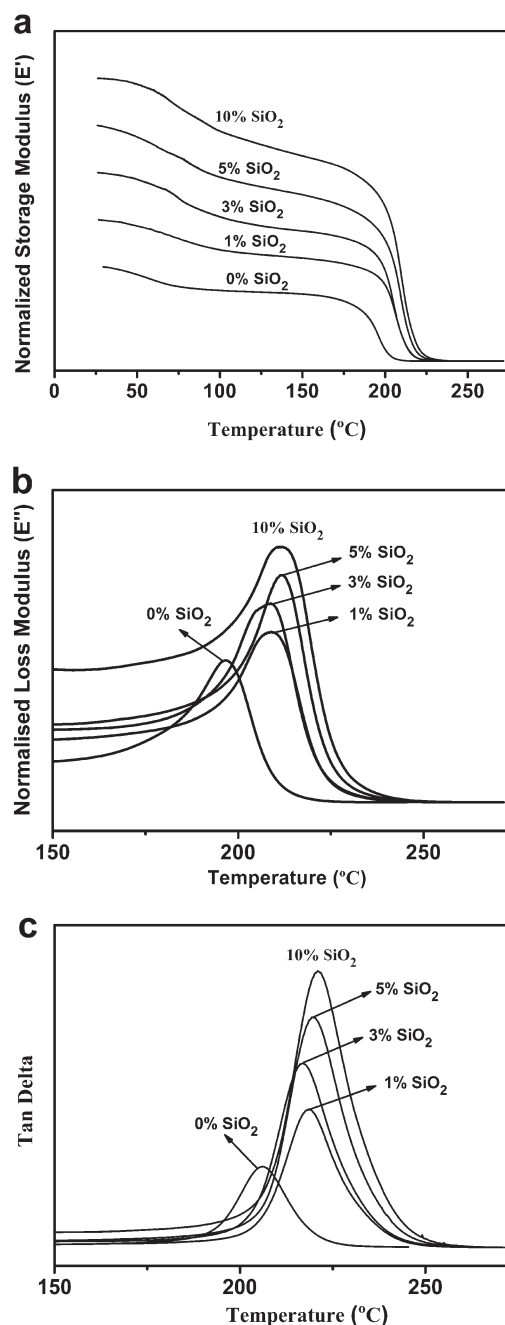
**Table I.** Mechanical Properties of the Pure and SiO<sub>2</sub>-Filled Epoxy Foams

Sample	SiO <sub>2</sub> (wt %)	Density (kg m <sup>-3</sup> )	Strength (MPa)	Modulus (MPa)	Specific strength (MPa m <sup>3</sup> kg <sup>-1</sup> )
EF	0	330 ± 13	5.85 ± 0.78	227.4 ± 25.6	0.0177 ± 0.0016
EF-1	1	363 ± 3	9.18 ± 0.07	307.2 ± 27.6	0.0253 ± 0.0002
EF-3	3	355 ± 4	8.49 ± 0.47	306.1 ± 22.6	0.0239 ± 0.0011
EF-5	5	349 ± 2	6.35 ± 0.11	284.9 ± 14.8	0.0182 ± 0.0002
EF-10	10	352 ± 5	7.41 ± 0.40	338.3 ± 11.5	0.0211 ± 0.0007

compressive force.<sup>17,31</sup> Compared with EF-5 and EF-10, the effect of high filler content on mechanical properties is dominant because of similar pore morphology.

### Thermal Stability of the Epoxy Foams

DMA is generally recognized to be sensitive to molecular motions and useful for evaluating subtle transitions occurred in polymeric system.<sup>32,33</sup> Figure 6 shows the dynamic mechanical properties of pure epoxy foams. The results show that the modulus decreases gradually with increasing temperature until a sharp decrease, which is attributed to the glass transition at 206°C. One of the most fundamental measurements made on polymeric materials is the measurement of the glass transition temperature ( $T_g$ ). In general,  $T_g$  can be measured using different viscoelastic parameters including the onset point of storage modulus ( $E'$ ), loss modulus ( $E''$ ) peak or  $\tan \delta$  peak.<sup>34</sup> The dependence of  $E'$ ,  $E''$ , and  $\tan \delta$  on temperature for the epoxy foam with various SiO<sub>2</sub> content is shown in Figure 7. Three kinds of glass transition temperature ( $T_{g-E'}$ ,  $T_{g-E''}$ , and  $T_{g-\tan \delta}$ ) are calculated through corresponding viscoelastic parameters, and listed in Table II. By comparison,  $T_{g-E'}$  occurs at the lowest temperature and relates to the start of mechanical failure.  $T_{g-E''}$  occurs at the middle temperature and is more closely related to the physical property changes attributed to the glass transition.  $T_{g-\tan \delta}$  occurs at the highest temperature and is normally used in literatures.<sup>35</sup> In any case, the  $T_g$  increases by about 11–15°C in comparison with pure epoxy foams. The glass transition temperature of a polymer corresponds to the onset of significant segmental chain motion, which is sensitive to the local environment of the polymer chains.<sup>36</sup> Due to the interaction between

**Figure 6.** Dynamic mechanical behavior of pure epoxy foam.**Figure 7.** Temperature dependence of  $E'$ ,  $E''$ , and  $\tan \delta$  for epoxy foam with various SiO<sub>2</sub> concentrations.

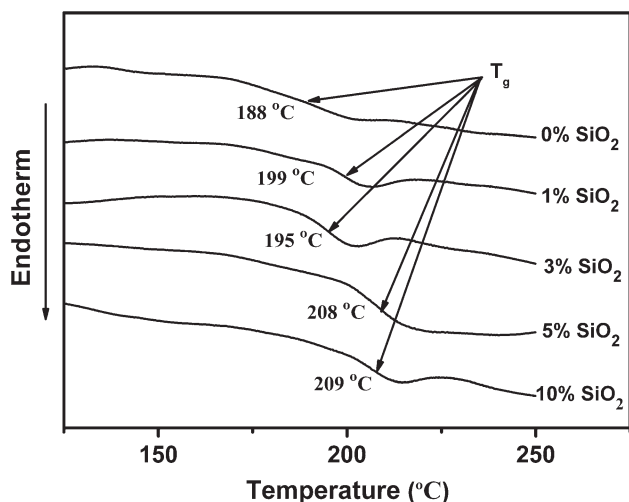
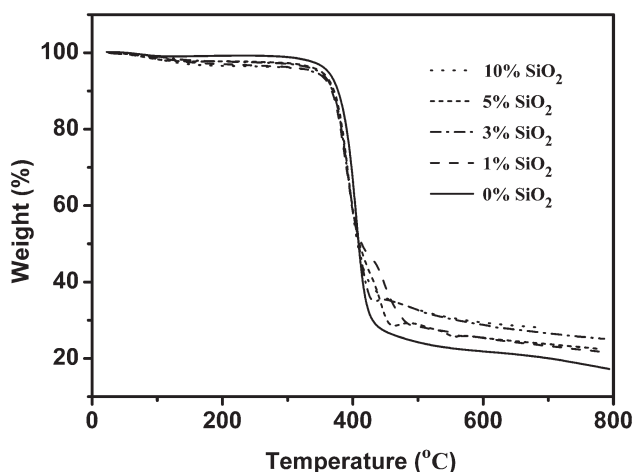
**Table II.** The Glass Transition Temperatures of Silica/Epoxy Foams via DSC and DMA

SiO <sub>2</sub> content (wt %)	0%	1%	3%	5%	10%
$T_{g-DSC}$ (°C)	188	199	195	208	209
$T_{g-E'}$ (°C)	185	199	197	203	202
$T_{g-E''}$ (°C)	197	209	209	212	211
$T_{g-tan \delta}$ (°C)	206	219	217	220	221

polymer chains and SiO<sub>2</sub>, most of the polymer chains are immobilized as an interface layer around the particles, and consequently the interfacial effects dominate the bulk properties of the material. Therefore,  $T_g$  of the composites has been shifted to higher temperature. This suggests that these composite foams possess very fine grain and high degree of dispersion. These results agree well with previous reports.<sup>37–39</sup>

DSC was also performed to characterize the thermal property of epoxy foams. As shown in Figure 8, the DSC curve of pure epoxy foam shows a  $T_{g-DSC}$  of around 188°C, and the glass transition temperature increases with increasing the content of SiO<sub>2</sub>. The data that calculated from DSC is much lower than that evaluated from the  $E''$  peak and  $\tan \delta$  peak of DMA curves, while it approaches  $T_{g-E'}$ , as shown in Table II. The main reason may be that DMA is corresponding to the dynamic modulus changes in matrix, which is more sensitive to environment temperature, while DSC is corresponding to the exothermic effect, only a small amount of heat releases during glass transition for polymer.<sup>35</sup> However, they show similar tendency, that is, the glass transition temperature increases with the content of SiO<sub>2</sub>.

The typical TGA curves of epoxy foams are presented in Figure 9, the results clearly indicate that all epoxy foams have similar decomposition temperature. The initial decomposition temperature, which is the onset of weight loss taken at 5%, and the peak decomposition temperature are about 363 and 406°C, respectively. The solid residues percentage after reaching 700°C for the pure epoxy foam is 20.1 wt %, which is attributed to the

**Figure 8.** Glass transition temperature ( $T_{g-DSC}$ ) of epoxy foams with different SiO<sub>2</sub> contents characterized by DSC.**Figure 9.** TGA curves of the epoxy foams.

formation of residual carbon.<sup>40</sup> Meanwhile, the solid residues yield increases proportionally with increasing the content of SiO<sub>2</sub>. These results indicate the epoxy foams possess outstanding thermostability.

## CONCLUSIONS

Steady shear viscosity of the DGEBA/DGEBS/DDS reacting mixture during the isothermal cure was determined from 140 to 190°C. All samples show an extremely rapid increase in viscosities after a critical time. The optimum precured temperature and time are 140°C and 50 min, respectively. Dynamic rheological measurements of the resin containing 0–5 wt % of SiO<sub>2</sub> were performed at various frequencies (1, 3, 5, and 10 Hz). The results clearly show that the gel points, measured by the crossover of  $\tan \delta$  curves with different frequencies, become independent of the frequency and decrease with increasing the content of SiO<sub>2</sub>.

The influence of SiO<sub>2</sub> content on the morphology, mechanical and thermal properties of epoxy foams was also investigated. The nucleating effect of SiO<sub>2</sub> during foaming process will increase the number of bubbles per volume unit and decrease its average cell size, which is in favor of mechanical property of epoxy foams. However, with an excess of nucleating point, the adjacent bubbles are collapsed to some extent, that is, large cells are surrounded by much smaller cells. The analysis of DMA indicates that the  $T_{g-tan \delta}$  of pure epoxy foam is as high as 206°C, and the incorporation of SiO<sub>2</sub> can significantly improve the  $T_g$  by above 11–15°C, since the interaction between polymer chains and SiO<sub>2</sub> results in the cooperative motion of the matrix polymer precipitously decreases. These results indicate that the epoxy foams have excellent thermal stability and mechanical properties, which describes a range of potential applications in naval vessels, military vehicles and aircraft.

## ACKNOWLEDGMENTS

The authors thank Buyi Li, a postdoctor of the Department of Chemistry, University of Liverpool, for fruitful discussions. We also greatly appreciate the financial support by the National Nature Science Foundation of China (Nos. 51273183 and 51173174) and

the Founder's Foundation of Institute of Chemical Materials, China Academy of Engineering Physics (No. 626010943).

## REFERENCES

1. Yan, D.; Dai, K.; Xiang, Z.; Li, Z.; Ji, X.; Zhang, W. *J. Appl. Polym. Sci.* **2011**, *120*, 3014.
2. Zhu, M.; Bandyopadhyay-Ghosh, S.; Khazabi, M.; Cai, H.; Correa, C.; Sain, M. *J. Appl. Polym. Sci.* **2011**, *124*, 4702.
3. Cao, X.; James Lee, L.; Widya, T.; Macosko, C. *Polymer* **2005**, *46*, 775.
4. Fabrizio, Q.; Loredana, S.; Anna, S. E. *Mater. Lett.* **2012**, *69*, 20.
5. Devi, K. A.; John, B.; Nair, C. P. R.; Ninan, K. N. *J. Appl. Polym. Sci.* **2007**, *105*, 3715.
6. Li, G.; Jones, N. *Compos A* **2007**, *38*, 1483.
7. Kim, H. S.; Oh, H. H. *J. Appl. Polym. Sci.* **2000**, *76*, 1324.
8. Benderly, D.; Rezek, Y.; Zafran, J.; Gorni, D. *Polym. Compos.* **2004**, *25*, 229.
9. Gupta, N.; Nagorny, R. *J. Appl. Polym. Sci.* **2006**, *102*, 1254.
10. Mcelhanon, J. R.; Russick, E. M.; Wheeler, D. R.; Loy, D. A.; Aubert, J. H. *J. Appl. Polym. Sci.* **2002**, *85*, 1496.
11. Zhong, F.; He, J.; Wang, X. *J. Appl. Polym. Sci.* **2009**, *112*, 3543.
12. Stefani, P. M.; Barchi, A. T.; Sabugal, J.; Vazquez, A. *J. Appl. Polym. Sci.* **2003**, *90*, 2992.
13. Alonso, M. V.; Auad, M. L.; Nutt, S. *Compos A* **2006**, *37*, 1952.
14. Alonso, M. V.; Auad, M. L.; Nutt, S. R. *Compos. Sci. Technol.* **2006**, *66*, 2126.
15. Alonso, M. V.; Auad, M. L.; Sorathia, U.; Marcovich, N. E.; Nutt, S. R. *J. Appl. Polym. Sci.* **2006**, *102*, 3266.
16. Stefani, P. M.; Perez, C. J.; Alvarez, V. A.; Vazquez, A. *J. Appl. Polym. Sci.* **2008**, *109*, 1009.
17. Stefani, P. M.; Cyras, V.; Barchi, A. T.; Vazquez, A. *J. Appl. Polym. Sci.* **2006**, *99*, 2957.
18. Takiguchi, O.; Ishikawa, D.; Sugimoto, M.; Taniguchi, T.; Koyama, K. *J. Appl. Polym. Sci.* **2008**, *110*, 657.
19. Corcuera, M. A.; Mondragon, I.; Riccardi, C. C.; Williams, R. J. *J. Appl. Polym. Sci.* **1997**, *64*, 157.
20. Grillet, A. C.; Galy, J.; Pascault, J.; Barin, I. *Polymer* **1989**, *30*, 2094.
21. Hou, T. *J. Appl. Polym. Sci.* **1990**, *41*, 819.
22. Cheng, K.; Chiu, W.; Hsieh, K.; Ma, C. *J. Mater. Sci.* **1994**, *22*, 887.
23. Winter, H. H. *Polym. Eng. Sci.* **1987**, *27*, 1698.
24. Boey, F. Y. C.; Qiang, W. *J. Appl. Polym. Sci.* **2000**, *76*, 1248.
25. Kahlweit, M.; Strey, R.; Busse, G. *J. Phys. Chem.* **1990**, *94*, 3881.
26. Sharma, M. K.; Shah, D. O. Macro- and Microemulsions; ACS Symposium Series. American Chemical Society: Washington, DC, **1985**; 18 pp.
27. Karthikeyan, C. S.; Sankaran, S.; Kumar, M. N. J.; Kishore J. *J. Appl. Polym. Sci.* **2001**, *81*, 405.
28. Wang, H.; Bai, Y.; Liu, S.; Wu, J.; Wong, C. P. *Acta Mater.* **2002**, *50*, 4369.
29. Kawaguchi, T.; Pearson, R. A. *Polymer* **2003**, *44*, 4229.
30. Kawaguchi, T.; Pearson, R. A. *Polymer* **2003**, *44*, 4239.
31. Lei, S.; Guo, Q.; Zhang, D.; Shi, J.; Liu, L.; Wei, X. *J. Appl. Polym. Sci.* **2010**, *117*, 3545.
32. Kim, J. W.; Park, S.; Harper, D. P.; Rials, T. G. *J. Appl. Polym. Sci.* **2013**, *128*, 181.
33. Lazaridou, A.; Biliaderis, C. G.; Kontogiorgos, V. *Carbohydr. Polym.* **2003**, *52*, 151.
34. Turi, E. A. Thermal Characterization of Polymeric Materials; Academic Press: New York, **1997**; 980 pp.
35. Zhang, R.; Li, R.; Lu, A.; Jin, Z.; Liu, B.; Xu, Z. *Polym. Int.* **2013**, *62*, 449.
36. Iqbal, A.; Frommann, L.; Saleem, A.; Ishaq, M. *Polym. Compos.* **2007**, *28*, 186.
37. Kotsilkova, R.; Fragiadakis, D.; Pissis, P. *J. Polym. Sci. Part B: Polym. Phys.* **2005**, *43*, 522.
38. Zhang, H.; Su, Z.; Liu, P.; Zhang, F. *J. Appl. Polym. Sci.* **2007**, *104*, 415.
39. Arrighi, V.; McEwen, I. J.; Qian, H.; Serrano Prieto, M. B. *Polymer* **2003**, *44*, 6259.
40. Lin, S.-T.; Huang, S. K. *Eur. Polym. J.* **1997**, *33*, 365.